Modeling, reconfiguration and loss modeling of multi-drive propulsion system under inverter faults in all-electric ships

Arshiah Y. Mirza
Electrical and Computer Engineering,
University of Connecticut
Storrs, CT, USA
arshiah.mirza@uconn.edu

Joshua Dupont
Mechanical Engineering,
University of Connecticut
Storrs, CT, USA
joshua.dupont@uconn.edu

Ali M. Bazzi
Electrical and Computer Engineering,
University of Connecticut
Storrs, CT, USA
bazzi@uconn.edu

***Abstract*— This article models an all-electric ship as a multidrive marine propulsion system from an electromechanical perspective and evaluates the overall losses in the system at various inverter faults. The model can be divided into electric drive controls modelling and the actual ship model. The electrical drive part of the model consists of the supervisory controller and electrical motor drives along with all its losses, while the ship model accounts for the hull resistance loss, thrust power calculations and the propeller losses for a YP yard patrol craft. Losses of the multi-drive propulsion system are evaluated under normal-mode and limp-mode operation and the impact of faults and reconfiguration of load on system losses are studied.**

***Index Terms*— All-electric ships, multi-drive propulsion systems, electric ship model, inverter fault, loss model**

I. INTRODUCTION

The history of electric propulsion drives dates to early 1900s when Emmet at General Electric proposed two electric drives - the first being a hybrid electric/steam turbine combination, the other a pure turboelectric drive in Transactions of the Society of Naval Architects and Marine Engineers [1]. Electric propulsion drives were also used in World War II; for examples, submarines in the US L-class, British R-class, German XXI-class, Japanese I-200 class, and others had a large amount of lead-acid batteries and several DC-motor propellers [2]. The latter half of the century saw nuclear power, computers, and precision-guided rocketry greatly increase the capabilities of naval warships. While the technologies improved through the decades, the next evolution in ship design has altered naval maritime. This next evolution in called advanced electrical power systems (AEPS) which involves the conversion of all shipboard systems to electric power [3].

Controls, distribution, energy storage, generators, motors, prime movers, and power converters form the crux of an all-electric ship (AES) driveline. They affect size, cost, fuel economy, space, performance, efficiency, power density, operating range, cooling requirements, current capacity, operating temperature, maintenance, fault management, system response, system reconfiguration, reliability and safety of all-electric ships [4].

Harvey and Thau [5] substantiated that AES are advantageous when compared to the conventional ship drives. The electrical transmission of power from prime mover has the simplest, most elastic, flexible and most reliable method of speed reduction. AES have better fuel economy - the fuel consumption for direct connected turbines drives (USS Idaho) is 20 - 47.8% more than turbo-electric transmission (USS New Mexico). Weight of AES when compared to ships with diesel drives vary considering overload capacity of electrical apparatus, factor of safety and flexibility of reserve. Spatial arrangement of drive in a ship is easier with non-electric drives when compared to AES since position of main generator and propelling motor is not rigid. Cost of AES does not vary largely when compared to other types of drive for a given torque and speed, but initial cost has a direct impact on the earning power of a ship due to interest, depreciation and insurance charges. Even if the initial investment on AES happens to be higher, the costs of piping shafts, oiling systems and maintenance offsets the extra cost in the long run. AES are easier to maintain as there are usually no large vales, thus only one man is required to operate the ship. When compared to other drives which involve fuel tanks and valves in diesel drives, maintenance of AES is easier as the only parts that wear down are bearings. Performance of AES is better when compared to other drives as the mechanical properties of motors are well suited to the propulsion applications. AES can cruise at higher speeds and decelerate to halt in comparatively lesser time. With efficient sensors, accurate and constant measurement of output power is possible in AES. They also accommodate very well, any changes in temperature and pressure when compared to diesel drives. When more than one electric drive (multi-drive) is incorporated, any faults or failure in one drive will reconfigure

This material is based upon work supported by the National Science Foundation under Grant No. 1752297

the propulsion system to limp-mode and ensure reliable and safe operation.

Though the electric propulsion systems in AES follow similar principles of electric drivetrains in electric vehicles (EVs), due to enormity and complexity of ships, there are multiple facets to be examined for a ship propulsion system in AES for an existing solution for electric drive-trains in EVs. Thus, research on AES is yet to mature.

This paper focuses on modeling the ship as a multi-drive propulsion system. The loss model comprises - electric drive losses and ship losses mechanical. The electric drive modeling consists of electric drive – inverter, controller and motor and mechanical modeling considers – hull resistance modeling, thrust power calculations and propeller losses. Overall, mathematical models of inverter, motor, ship and propeller are considered. The impact of inverter faults and system reconfiguration is evaluated for system loss.

Section 2 gives a thorough literature review of ship modeling approaches. Section 3 describes the ship hull resistance model. Section 4 describes modeling of induction motor drives and results of implementation of the IFOC on the drives during fault conditions. Section 5 gives the power loss curves of the model at normal and limp-mode operations. Section 6 concludes the paper.

II. Modeling of All-Electric Ships

Due to enormity and complexity of ships, AES is viewed from different perspectives by researchers across the world. All the modeling methods and techniques can be broadly categorized into any one or a combination of any of three basic aspects of ship: mechanical [6-19], thermal [20-30] and electrical [31-67]. Thus, modeling of AES is focused on many branches of research as shown below:

A. Mechanical modeling of AES:

Shipbuilding is a practice dating back tens of thousands of years, beginning with simple canoes made from carved out tree trunks to massive seagoing vessels of the modern day. Since then, a lot of thought and research has gone into mechanical aspects of ship building. Mechanical modeling of ships can be done by:

a) Computational fluid dynamics: Models developed using this method is accurate, and model is obtained by solving complex differential equations of fluids equations numerically but requires detailed information on hull form [6-11].

b) Empirical models: These models are based on dimensional analysis and mostly preferred since they require comparatively little information. The equations are derived from experimental towing-tank data and dimensional analysis. Extensive data collection was done between 1970 and 1990 [13-19].

B. Thermal modeling of AES:

Devices integrated in AES for control, power, propulsion, and weapon systems produce heat which affect the ship performance. To avoid catastrophic system breakdowns due to excessive heat, AES should be designed to comply with the cooling requirement of all the devices. Thermal modeling of AES has been studied in [20-28], shipboard processes [29-30] devices and loads have been studied. These studies give insight during early design and development stages of effective ship cooling networks. Thus, system level simulations permit the analysis of the overall ship thermal behaviors under different operation modes, ambient conditions, load capacity, performance enhancement etc., and help us plan suitable ship thermal management strategies.

C. Electrical modeling of AES:

As integration of electric propulsion drive is a newer concept when compared to mechanical built and thermal modeling. Replacing the conventional diesel engine drive with electric drives gives rise to multiple opportunities and challenges. The key areas of electrical modeling are:

a) Power electronics and drives: AES is powered through electric propulsion-drive, and thus can be modelled as an electric-drive or a multiple electric drives (multi-drive) which encompasses a DC source, inverter, controller and motor in each drive. Multilevel inverters are the key enablers in electric drive trains for AES[31-33]. As the voltage handling capacity of inverters increased with multilevel inverters, they could be used in ships to harness the DC power available to run the motor on the drive at desired speed. Research on inverters involves analysizing topologies of multi-level inverters[32], high-power and high-frequency switching[35]. As SiC and GaN devices with higher voltage capabilities enter the market, the scope for improvement in this area seems very promising. The various motors, motor drives and controllers used in AES [36,37] are usually application specific and depend on size, weight, speed and load capacity of AES. A careful choice of high-voltage high-frequency inverters, and efficient power drives, with intelligent controllers can reduce the size of ship and improve the performance of the AES considerably. In addition to modeling the drives, modeling faults and thier diagnosis, prognosis and recovery in inverter, motor, and sensors can lead to reliable, safe and smooth maintenance of AES [38-41].

b) Power systems: Owing to the large amount of power generated, transmitted and distributed, AES are generally viewed as power system and more specifically as a microgrid since they are islanded from a grid network. Many models of AES have been simulated in [42-51]. Power systems on AES have limited generation capacity and smaller rotating inertia compared to large power systems and the generators can be easily overloaded at sudden load changes. Nonlinear and dynamic loads in AES are large relative to the total generation capacity and reduce the stability margin[52-55]. Moreover, pulse loads, which are very common in AES, draw a large amount of power in a short period of time and cause significant frequency and voltage oscillations. Thus, an effective power system model and load model are necessary for real-time load management technique to achieve load and generation balancing [56-65].

c) Control theory - Stability and transients: As control systems and actuators are integrated in the broad electrical,

mechanical and thermal ship-board processes in AES, instability in any of the tuning and control parameters while normal operation may lead to fatal disasters. Thus, analysis of stability and transients in drive operation, reconfiguration, load sharing and management is necessary [43,68].

d) Stochastic models of ship: AES have a innumerous uncertain parameters. Modeling those parameters in AES as random variables incorporates the uncertainities. For example, models of ship power systems [34,55], operations efficiency of multi-drives [66] have been incorprated. Also, many machine learning algorithms are implemented to track the targets for AES specific to warfare [67].

This paper focuses on modeling the electric drives in AES from a power electronics and drives perspective and the mechanical model of the ship hull using empirical model. Factors such as air resistance, wind, ocean currents, and swells were not considered in the mechanical model. Each of the two drives on the ship have been modelled using indirect field-oriented controller (IFOC), a 3-phase hex-bridge inverter, an induction motor attached to a propeller. The load is shared between both the drives under normal operation. The model of multidrive marine propulsion system is shown in Fig. 1. In addition to modeling, 3 inverters faults have been simulated. When an inverter fault occurs, the system reconfigures to limp-mode operation. Under limp-mode operation, the entire load which was initially shared between both the drives is now shifted to drive 2.

III. AES - MECHANICAL MODEL

J. Holtrop and G.G.J Mennen developed an empirical model to approximate the coefficients and model the hull resistance of ship. This model was developed along the guidelines set forth by the international tank towing conference (ITTC) of 1957 [69] after performing a series of towing experiments for 200 hull forms in still water. This paper models a ship hull of a US Navy Yard Patrol boat [70]. It is also assumed that the vessel moves only forwards through calm water, and that the rudder can fully compensate for imbalances in drive-shaft torques (load sharing). Table-B gives the ship and water parameters.

A US Navy Yard Patrol boat is shown in Fig 1. These ships have 2 drives and each drive has an advertised engine power of 715 BHP and a rated speed of 12.6 knots [70]. This speed can also be observed in Fig. 2 (marked with a green star), where the hull resistance drops validating the model developed below.

Fig. 1. US Navy Yard Patrol boat YP 703.

A. Hull resistance model

Using the parameters of Table-I into US Navy Yard Patrol boat model, the hull resistance model is developed at different ship velocities as shown in Fig. 2.

As a ship moves forward, it must push the water in front of it aside. The total force required to do this is called the total hull resistance (R_T) of the ship. Hull resistance is a complex phenomenon dependent on several physical factors. These include ship velocity, shape of its hull, and fouling of the hull (corrosion and the growth of barnacles) and can be written as

$$R_T = R_V + R_w + R_A \quad (1)$$

Through dimensional analysis, these three resistances may be written as dimensionless coefficients in the form as

$$C_T = C_V + C_w + C_A \quad (2)$$

where (for each C and R component):

$$C = \frac{R}{\frac{1}{2}pV^2S} \quad (3)$$

here $\frac{1}{2}pV^2$ is the dynamic pressure of the fluid traveling past the hull [71].

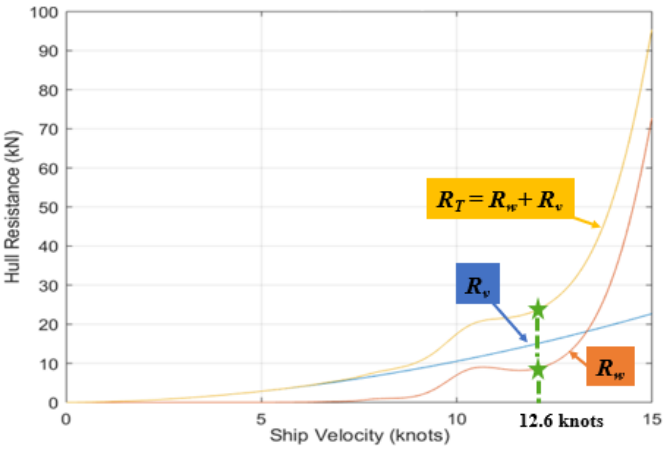

Fig. 2. Hull resistance of US Navy Yard Patrol boat YP 703 using Holtrop-Mennen model

B. Thrust Power model

Once the R_T versus velocity curve for a particular ship is determined, it is possible to find the power required to propel the ship forward with constant speed. The effective towing power (P_E) is the power needed to pull (via a cable) a ship forward [71]:

$$P_E = R_T V_s \quad (4)$$

Typically however, P_E is found to be less than the actual power required for a ship to propel itself through the water. This is due to the effects of the propellers on the hydrodynamics of the ship [71]. When a propeller is active, it pulls more water underneath the hull, increasing the magnitude of the water's flow rate relative to the hull. The result is a reduction in both stern pressue and the pressure along the bottom of the hull.

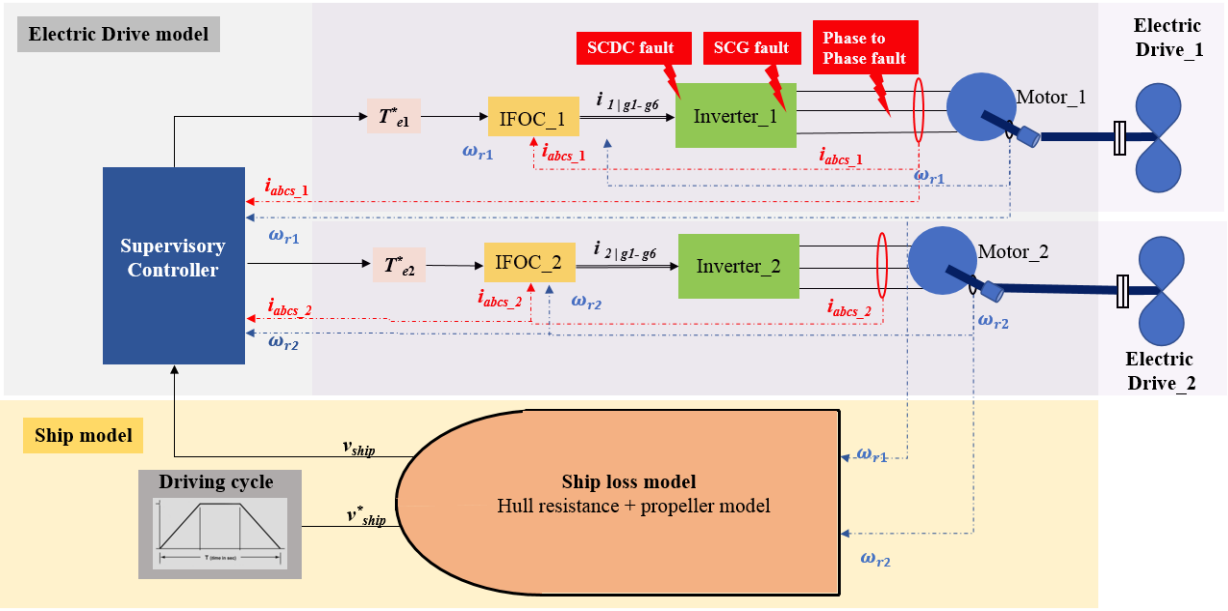

Fig. 3. AES multi-drive propulsion system model

The former causes an additional rearwards force, while the latter causes the vessel to increase its draught in the water. This additional resistance may be accounted for with the use of another dimensionless coefficient, the thrust deduction coefficient (t), defined as:

$$t = \frac{F_s}{F_T} = \frac{F_T - R_T}{F_T} \qquad (5)$$

where F_s is the additional force due to the action of the propeller, and F_T is the total thrust delivered by the propeller. (5) can then be rewritten to obtain:

$$F_T = \frac{R_T}{(1-t)} \qquad (6)$$

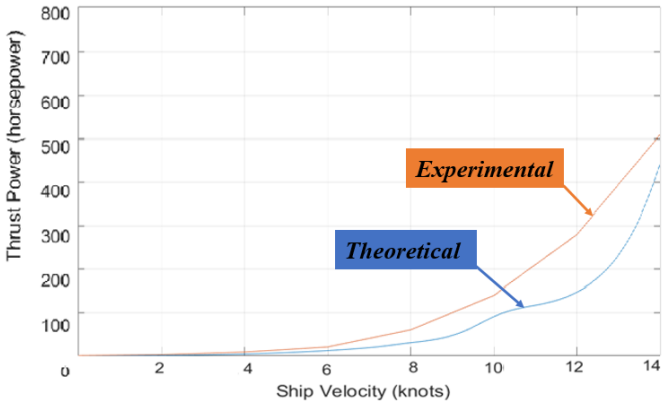

Fig 4. Thrust power required for US Navy Yard Patrol boat YP 703

Additionally, the horizontal speed of the propeller itself, relative to the surrounding water, is not the same as that of the ship [71]. As the ship moves forward, it drags water alongside it, resulting in a wake in which the ship's propellers operate. The speed propeller relative to the water immediately surrounding it is therefore less than the ship's actual speed (relative to still water). A propeller's speed of advance, V_a is thus defined as the propeller's linear speed relative to the ship's wake [71]. V_a is related to ship speed via the wake coefficient (w) as

$$V_A = V_S * (1 - w) \qquad (7)$$

w and t are approximated for a twin propeller ship using Holtrop and Mennen's model [69]. The total thrust power (P_T) delivered by the two propellers is:

$$P_T = F_T V_a = \frac{R_T}{(1-t)} * V_S(1-w) \qquad (8)$$

$$P_T = R_T V_S \frac{1-w}{1-t} = \frac{P_E}{\eta_H} \qquad (9)$$

where the denominator η_H is the hull efficiency of the vessel ($\eta_H = \frac{1-t}{1-w} = \frac{P_E}{P_T}$) [71]. Using this relation alongside the hull resistance model, the graph of thrust power P_T as a function of ship velocity (V_s) is plotted for two different vessels in Fig. 4.

IV. Multi-Drive Propulsion System Model

As the maximum thrust power required for each drive in US Navy Yard Patrol boat does not exceed 500HP (shown in Fig. 4) and at rated speed the thrust power equals 150 HP. The electric drive is suitably sized and modeled to be propelled by two 500-HP inverter fed motor drives instead of diesel engines (Originally, Navy Yard Patrol boat YP703 is propelled by 2 category C-18 diesel engines). To ensure reliability and improve the fuel efficiency during travel, two propulsion drives are run parallelly for load sharing. The schematic of multi-drive AES modeled in this paper is shown in Fig. 3.

A. Motor drive model

The multi-drive model has been modeled as in described [73].

a) Induction motor model

[37] describes the motors used in AES. Among the motors listed, induction motors are chosen for modeling since they are widely used in industry due to their ruggedness and ease of

maintenance. The motors are 3 phase, 4 pole, 500 HP induction machines and controlled via indirect field-oriented control (IFOC).

One of the main advantages of induction machines is that they are physically simple and tend to be quite rugged. These advantages carry through to ship propulsion as they do not have commutator nor slip rings to demand maintenance, and aside from the main shaft bearings, they are easy to maintain. The control of induction motors has become very flexible with vector control techniques which control the torque and flux independently [72]. The induction motor model has been modeled similarly as in [73].

b) Inverter Model

Each of these drives is shafted directly to a propeller. The motor drive includes a 2.3kV inverter, fed from a 3500V DC source.

c) Load model

A quadratic load is considered with motor torque proportional to square of its speed ($T_e \, \alpha \, \omega^2$).

B. Normal operation

To model the normal operation, drive 1 and 2 are modelled healthy without any faults. During the normal operation, both the drives power AES, and the load is shared. To show the normal operation of drives, a 500Nm load torque is demanded at 2 seconds on drives 1 and 2 with no load torques previosly. Since both the drives are identical at normal operation, only one waveform for a the parameter under study is shown. The corresponding phase A inverter voltage of one of the drives is shown in Fig. 5. The 3-phase motor currents (3 phase waveforms overlap in this case) are shown in Fig. 6 and Fig. 7 shows the motor speed. It can be seen that the drives track the changes according to the load demanded.

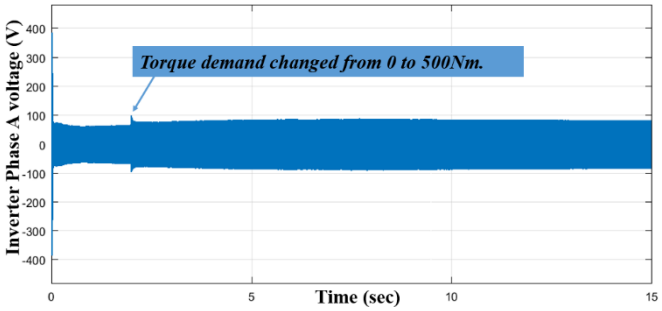

Fig. 5. Normal operation - Inverter phase-A voltage on drives 1 and 2

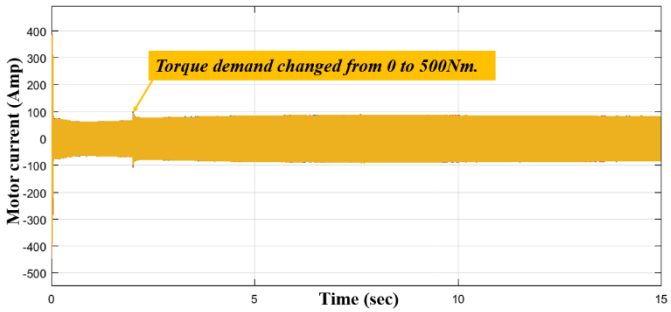

Fig. 6. Normal operation - Motor current - Phases A, B and C in drives 1 and 2

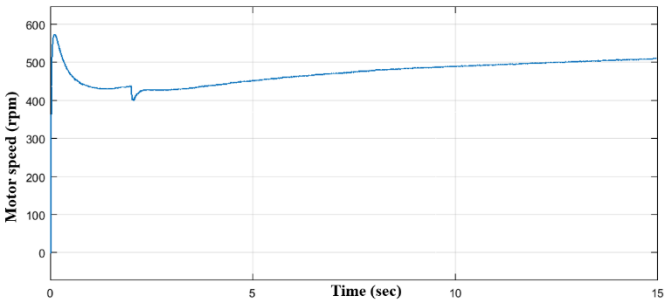

Fig. 7. Normal operation - motor speed in drives 1 and 2

C. Limp-mode operation - Fault modeling

Extensive research on faults and their diagnosis [74] has been carried out electric vehicles (EV). But the effects of faults in the drives and load sharing among the drives in marine propulsion systems have not been studied thoroughly. This paper models and implements 3 inverter faults as below:

- *Short Circuit Direct Current fault (SCDC):* Phase A of inverter shorted to positive DC rail at 7 seconds
- *Short Circuit to Ground fault (SCG):* Phase A of inverter shorted to ground at 10 seconds
- *Phase to Phase fault (PP):* Phase A of motor shorted to Phase B at 13 seconds

To model the fault and limp-mode, the above mentioned inverter faults are injected in drive-1 while drive-2 is healthy. When an inverter fault occurs on drive-1, the entire load is shifted to the healthy drive-2 and the multi-drive AES operates in limp mode operation with a limited availability of one drive. Here only drive-1 (faulty drive) waveforms are shown since, drive-2 remains healthy as shown in Fig. 5,6 and 7. Fig. 8 shows the 3-phase motor currents at faulty and limp mode operations while Fig. 9 shows the corresponding drive-1 motor speed. It can be seen that, the drive restores back to its normal operation after the faults are cleared. The inverter phase-A voltage is shown in Fig. 10. The magnitude of phase-to-phase fault voltage is very high in the order of megavolts, thus, a zoomed in version of inverter phase-A voltage is shown in fiugure 9 to observe the behavior at SCDC and SCG faults.

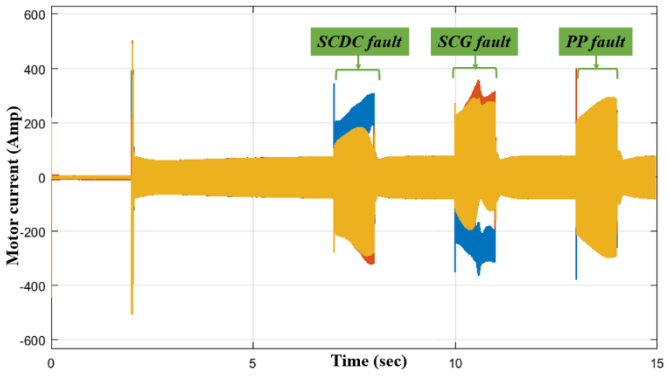

Fig. 8. Drive 1 - Motor current - Phases A, B and C

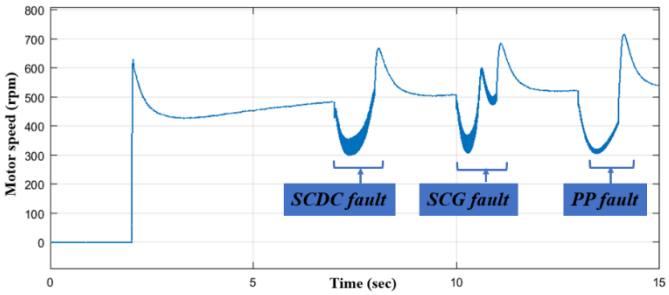

Fig. 9. Drive 1 - Motor Speed at faults

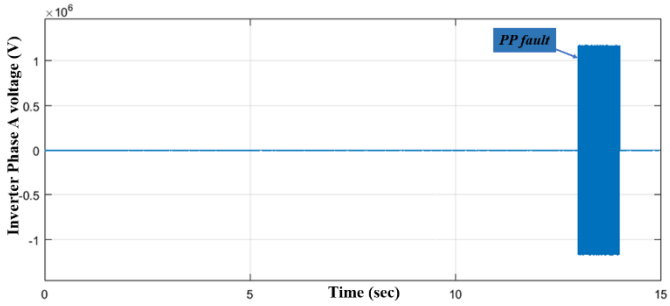

Fig. 10. Inverter phase – A Voltage

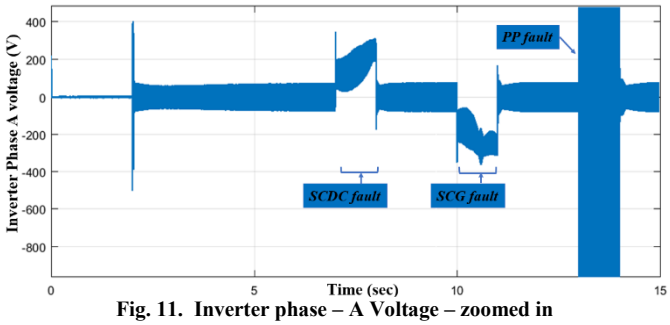

Fig. 11. Inverter phase – A Voltage – zoomed in

V. LOSS MODELING

A. Motor and inverter power loss model

The combined power loss models for inverter and induction motor for parameters are shown in the Fig. 12. Total drive loss in each drive at normal operation (purple) and limp-mode (yellow) will be a sum of the motor loss (blue), inverter loss (orange) as shown in Fig. 12.

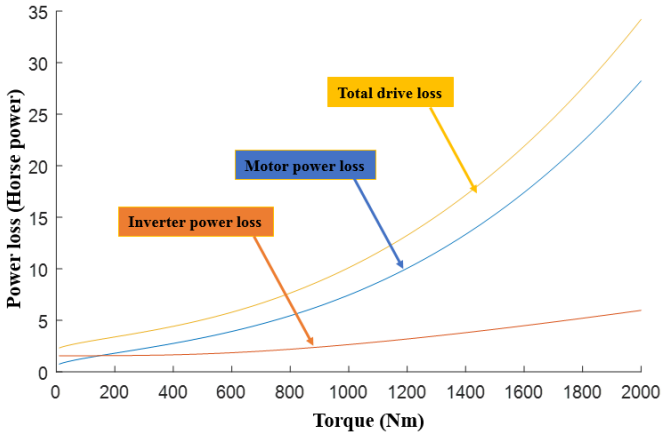

Fig. 12. Electric drive loss model at normal mode and limp-mode operation

B. Motor and inverter power loss model at normal and limp-mode operation:

The combined power loss models for inverter and induction motor at different modes of operation are shown in Fig. 14. Total drive loss in each drive at normal operation (purple) and limp-mode (yellow) will be a sum of the motor loss (blue), inverter loss (orange) as shown in Fig. 12.

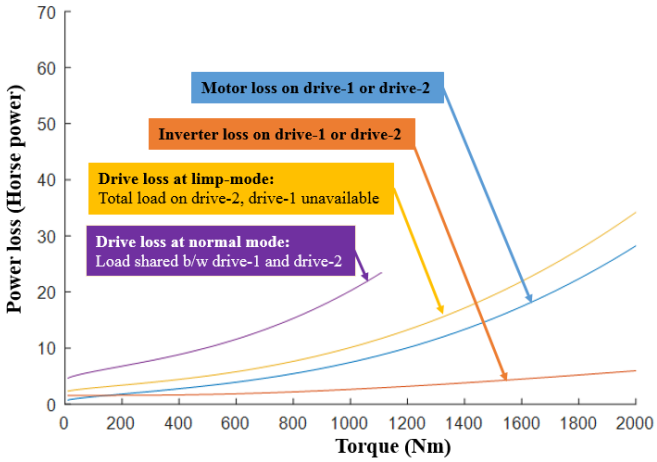

Fig. 13. Drive power loss at normal and limp-mode operation

For example, if a load on AES demands 1400 Nm, under normal operation, the load is shared between both the drives. Rated torque of the 500 HP induction motor modeled is 1980 Nm [75] which is more than the load demanded. Drive-1 supplies 700Nm and drive-2 supplies 700 Nm following the losses in normal-mode (orange curve) in Fig. 13, the drive losses are approximately 12 HP. In limp mode, drive-1 is disabled and drive-2 supplies the total load torque 1400 Nm and the drive loss is approx. 15.5 HP (blue curve) in Fig. 13. Though the losses are higher under limp-mode operation, AES still runs at a lesser availability.

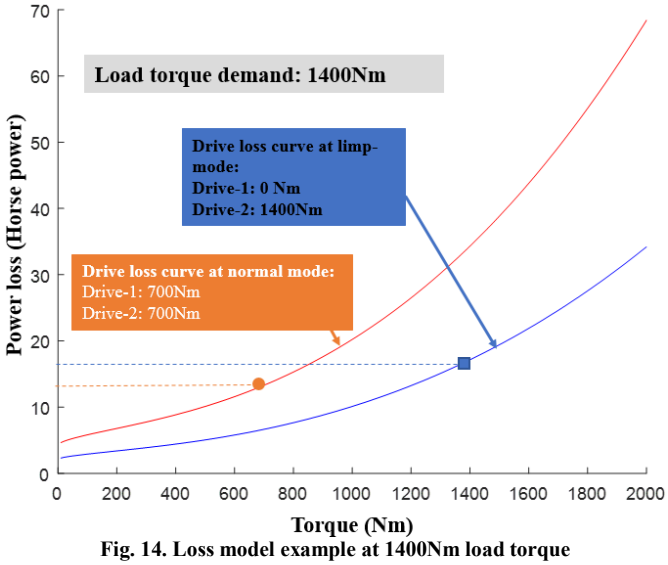

Fig. 14. Loss model example at 1400Nm load torque

C. Propeller power loss model

The first step is to determine propeller power loss is to find the thrust power required to propel the ship (Section III) and the output power from the electrical drive. The thrust power model for ship with parameters given in Table I was developed as shown in Fig. 15 and the output power from the electric drive has been modelled following [73] and shown in Fig. 15. Once, both the ship thrust power and power from the multi-drive are obtained, subtracting the ship's thrust power from the output power of induction motor drive yields propeller losses at different operating conditions.

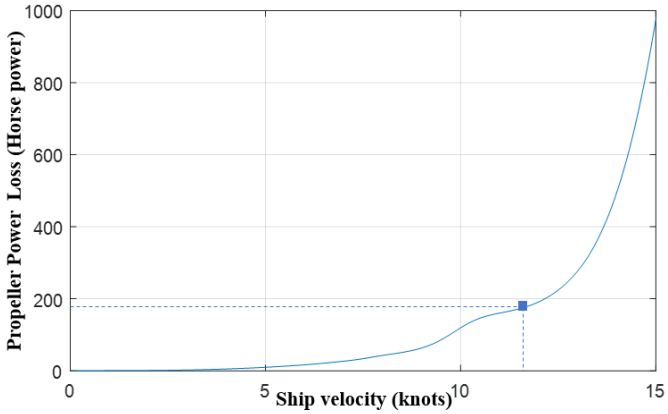

Fig. 15. Propeller loss

Based on the parameters given in table I, thrust power model for AES was developed as shown in Fig. 15. The combined power loss models for inverter and induction motor are shown in Fig. 12. Total drive loss in each drive will be a sum of the motor loss, inverter loss and the losses in the propeller.

VI. Conclusion

The AES has been modeled as a multi-drive and the mechanical properties ship have been modelled using empirical model. Faults in multi-drive were injected and ship operation under normal and limp-mode conditions were analyzed. The power loss models for AES (multi-drive and ship) were developed and the AES loss model was studied in different modes of operation.

Appendix

TABLE I. Ship Parameters

Parameter	***Acronym***	***Value***	***Units***
Seawater Kinematic Viscosity	γ	$9.37*10^{-7}$	m^3/s
Seawater Density	p	1023.6	kgs/m^3
Waterline Length	L (or L_{pp})	141.73	m
Waterline Beam	B	20.27	m
Draught	T	7.93	m
Propeller Diameter	D	3	m
Displacement	d	11,911	m^3
Midship-Area (Cross-section)	A	112.5	m^2
Ship Velocity	V_s	Variable	m/s

TABLE II. Induction Motor Parameters

Parameter	***Acronym***	***Value***	***Units***
Rated Power	P_r	500	Hp
Rated Speed	ω_r	1773	RPM
Voltage (Line to line)	V	2.3	kV
Rated Frequency	F	60	Hz
Rated Torque	T_r	1980	N.m

References

[1] C. E. Babb, "How we got here", Future force, Naval Science and Technology magazine, , Vol. 2, No. 3, Summer 2015

[2] E. Skjong, E. Rødskar, M. Molinas, T. A. Johansen and J. Cunningham, "The Marine Vessel's Electrical Power System: From its Birth to Present Day," *in Proc. 2015 IEEE,* Vol. 103, pp. 2410-2424

[3] T. Ericsen, "Advanced electrical power systems (AEPS) thrust at the office of naval research," *Proc. 2004 IEEE Power Engineering Society General Meeting,* Denver, CO, 2004, pp. 973

[4] S. P. Markle, (2017, Apr.) "Surface Navy Electrical Leap Forward", Sea-Air-Space Expo, [Online]. Available: http://www.navsea.navy.mil

[5] H. F. Harvey and W. E. Thau, "Electric Propulsion of Ships," in Transactions of the American Institute of Electrical Engineers, vol. 44, pp. 497-522, Jan. 1925

[6] P. Voxakis, "Ship Hull Resistance Calculations Using CFD Methods" Masters Thesis, Dept. Mech. Eng., Massachusetts institute of technology, MA, 2012

[7] D.Sridhar, T V K Bhanuprakash, H N Das, "Frictional Resistance Calculations on a Ship using CFD", *International Journal of Computer Applications,* vol. 11, no.5, 2010

[8] T. Tezdogan, Y. K. Demirel, P. Kellett, M. Khorasanchi, A. Incecik, O. Turan, "Full-scale unsteady RANS CFD simulations of ship behaviour and performance in head seas due to slow steaming", *Ocean Engineering*, Vol. 97, pp. 186-206, 2015

[9] Y. M. Ahmed, O. B. Yaakoba, M. F. A. Rashid, A. H. Elbatran "Determining Ship Resistance Using Computational Fluid Dynamics (CFD)", *Journal of Transport System Engineering,* vol 2, no.1, 2015

[10] M. Shahid and D. Huang, "Resistance Calculations of Trimaran Hull Form Using Computational Fluid Dynamics," *Proc. 2011 Fourth International Joint Conference on Computational Sciences and Optimization*, pp. 81-85

[11] D. Frisk, L. Tegehall, "Prediction of High-Speed Planing Hull Resistance and Running Attitude, A Numerical Study Using Computational Fluid Dynamics" M.S. thesis, Dept. of Shipping and Marine Tech, Chalmers University of Technology, Sweden, 2015

[12] A.S Gotman, "A method for calculating ship resistance components using a theoretical drawing" *International journal of applied and fundamental research* , no. 1, 2012

[13] S. Y. Jeong, K. Choi, K. J. Kang, J. S. Ha, "Prediction of ship resistance in level ice based on empirical approach," *International Journal of Naval Architecture and Ocean Engineering*, vol. 9, no. 6, 2017, pp. 613-623.

[14] J. Koto, E. Afrizal, "Empirical Approach to Predict Ship Resistance in Level Ice" *Journal of Ocean, Mechanical and Aerospace - Science and Engineering*, Vol.45, 2017

[15] "Methods of Determining Ship Resistance", A Review of Empirical and Numerical Methods to Determine Wave Resistance on Ship Hull [Online]

Available:https://homepages.cae.wisc.edu/~chinwu/CEE310_Fluid_Mechanics/Picture/Picture_of_the_week_2014/Shipres.html
[16] A. F. Molland, S. R. Turnock and D. A. Hudson *Ship Resistance and Propulsion: Practical Estimation of Ship Propulsive Power*, vol I. New York: Cambridge University Press, 2011
[17] J. Holtrop, G.G.J. Mennen, "Statisical power prediction method", *International Shipbuilding Progress,* vol. 25, pp. 253-256, 1978.
[18] J. Holtrop, G.G.J. Mennen, "An approximate power prediction method", *International Shipbuilding Progress*, vol. 29. pp. 166-170, 1982
[19] H.O. Kristensen, M. Lützen, "*Prediction of resistance and propulsion power of ships",* unpublished, Project No. 2010-56, Report No. 4.K, Denmark, 2013
[20] J. C. Ordonez et al., "Thermal management aspects of all-electric ships," *Proc. 2013 IEEE Electric Ship Technologies Symposium* (ESTS), Arlington, VA, 2013, pp. 55-61
[21] R. Fang, W. Jiang, J. Khan and R. D. "System-level thermal modeling and co-simulation with hybrid power system for future all electric ship," *Proc. 2009 IEEE Electric Ship Technologies Symposium*, Baltimore, MD, 2009, pp. 547-553
[22] A. R. Holsonback and T. M. Kiehne, "Thermal aspects of a shipboard integrated electric power system," *Proc 2010. IEEE International Conference on Automation Science and Engineering,* Toronto, ON, 2010, pp. 742-749
[23] S. Yang, J. C. Ordonez, J. V. C. Vargas, H. Babaee, J. Chalfant and C. Chryssostomidis, "Comprehensive system-level thermal modeling of all-electric ships: Integration of SMCS and vemESRDC," Proc *2015 IEEE Electric Ship Technologies Symposium*, Alexandria, VA, 2015, pp. 251-255
[24] J. A. Souza, J. C. Ordonez, J. V. C. Vargas and R. Hovsapian, "Control volume based thermodynamic modeling applied to the thermal management of a notional all-electric ship*," Proc. 2011 IEEE Electric Ship Technologies Symposium*, Alexandria, VA, pp. 161-166
[25] S. Liu and Y. Jia, "A modeling approach of Integrated Electrical-Thermal System for early ship design," *Proc. 2014 33rd Chinese Control Conference,* Nanjing, pp. 6256-6261
[26] T. M. Kiehne, "Dynamic assessment of thermal management strategies aboard naval surface ships," *Proc. 2011 IEEE Electric Ship Technologies Symposium*, Alexandria, VA, pp. 38-41
[27] F. G. Dias, J. A. Souza, J. C. Ordonez, J. V. C. Vargas, R. Hovsapian and J. V. Amy, "Notional all-electric ship thermal simulation and visualization," *Proc. 2009 IEEE Electric Ship Technologies Symposium*, Baltimore, MD, pp. 539-546
[28] M. O. Faruque, V. Dinavahi, M. Sloderbeck and M. Steurer, "Geographically distributed thermo-electric co-simulation of all-electric ship," *Proc. 2009 IEEE Electric Ship Technologies Symposium, Baltimore,* MD, pp. 36-43
[29] S. Yang, M.B. Chagas, J.C. Ordonez, "Modeling, cross-validation, and optimization of a shipboard integrated energy system cooling network", Applied Thermal Engineering, vol. 145, pp. 516-527, 2018
[30] R. Fang, W. Jiang, J. Khan and R. Dougal, "Thermal modeling and simulation of the chilled water system for future all electric ship," *Proc. 2011 IEEE Electric Ship Technologies Symposium*, Alexandria, VA, pp. 265-271
[31] K. Lentijo and K. Hobart, "Three-level inverter with 60 A, 4.5 kV Si IGBT/SiC JBS power modules for marine applications," Proc. *2013 IEEE Electric Ship Technologies Symposium*, Arlington, VA, pp. 162-165
[32] M. Spichartz, V. Staudt and A. Steimel, "Modular Multilevel Converter for propulsion system of electric ships," Proc. *2013 IEEE Electric Ship Technologies Symposium*, Arlington, VA, pp. 237-242
[33] L. Zhou, H. Liu, Y. Xu and L. Bai, "A multi-functional grid-connected inverter and its application in the all-electric ship," Proc. *2014 IEEE Conference and Expo Transportation Electrification Asia-Pacific*, Beijing, 2014, pp. 1-5.
[34] M. Derakhshanfard " Analysis of different topologies of multilevel inverters " M.S. thesis, Dept. of Energy and Environment, Chalmers University of Technology, Sweden, 2010
[35] J. D. Herbst, F. D. Engelkemeir and A. L. Gattozzi, "High power density and high efficiency converter topologies for electric ships," *Proc. 2013 IEEE Electric Ship Technologies Symposium*, Arlington, VA, pp. 360-365
[36] J. C. Dermentzoglou, "Investigating the incorporation of a doubly fed induction machine as a shaft generator into a ship's system: Application of a vector control scheme for controlling the doubly fed induction machine," Proc. *2014 International Conference on Electrical Machines (ICEM)*, Berlin, pp. 2319-2324
[37] J. L. Kirtley, A. Banerjee and S. Englebretson, "Motors for Ship Propulsion," in *Proc. of the IEEE*, vol. 103, no. 12, pp. 2320-2332, Dec. 2015
[38] W. Chen and A. M. Bazzi, "Fault Prognostics of Multilevel Inverters Using On-State Resistance Evolution," Proc. *2018 IEEE Energy Conversion Congress and Exposition (ECCE)*, Portland, OR, pp. 7292-7296
[39] W. R. Jensen, E. G. Strangas and S. N. Foster, "A Method for Online Stator Insulation Prognosis for Inverter-Driven Machines," in *IEEE Transactions on Industry Applications*, vol. 54, no. 6, pp. 5897-5906, Nov.-Dec. 2018
[40] A. Silva, A. M. Bazzi and S. Gupta, "Fault diagnosis in electric drives using machine learning approaches," *Proc. 2013 International Electric Machines & Drives Conference*, Chicago, IL, 2013, pp. 722-726
[41] Yi Lu Murphey, M. A. Masrur, ZhiHang Chen and Baifang Zhang, "Model-based fault diagnosis in electric drives using machine learning," *IEEE/ASME Transactions on Mechatronics*, vol. 11, no. 3, pp. 290-303, June 2006
[42] A. A. H. Mansour, "Harmonic Reduction of Islanded Microgrid Ships Using Fuzzy Controlled DCMLI," *Proc. 2018 Twentieth International Middle East Power Systems Conference*, Cairo, Egypt, pp. 152-156
[43] Zhaomin and Fanyinhai, "The Voltage Stability Research of Ship Electric Power System," Proc. *2006 CES/IEEE 5th International Power Electronics and Motion Control Conference*, Shanghai, pp. 1-5
[44] R. E. Crosbie, "Low-cost, high-speed, real-time simulation for electric ship power systems," Proc 2005, *IEEE Electric Ship Technologies Symposium,*, Philadelphia, PA, pp. 46-47
[45] S. J. Dale, "Ship power system testing and simulation," Proc. 2005 *IEEE Electric Ship Technologies Symposium,*, Philadelphia, PA, pp. 202-20
[46] A. Ouroua, L. Domaschk and J. H. Beno, "Electric ship power system integration analyses through modeling and simulation," Proc 2005, *IEEE Electric Ship Technologies Symposium,*, Philadelphia, PA, pp. 70-74
[47] Y. Xie, G. Seenumani, J. Sun, Y. Liu and Z. Li, "A PC-Cluster Based Real-Time Simulator for All-Electric Ship Integrated Power Systems Analysis and Optimization," Proc. *2007 IEEE Electric Ship Technologies Symposium*, Arlington, VA, pp. 396-401
[48] H. H. Zhu and Z. Dong, "Modeling and Simulation of Hybrid Electric Ships with AC Power Bus - A Case Study," *2018 14th IEEE/ASME International Conference on Mechatronic and Embedded Systems and Applications (MESA)*, Oulu, 2018, pp. 1-8
[49] K. L. Butler-Purry, G. R. Damle, N. D. R. Sarma, F. Uriarte and D. Grant, "Test Bed for Studying Real-Time Simulation and Control for Shipboard Power Systems," Proc. *2007 IEEE Electric Ship Technologies Symposium*, Arlington, VA, pp. 434-437
[50] S. Lee, S. Kim, Y. Jeong and S. Jung, "Power system modeling and analysis of electric ship propulsion system," Proc. *2009 - 31st International Telecommunications Energy Conference*, Incheon, 2009, pp. 1-4
[51] A. Zahedi and L. E. Norum, "Modeling and Simulation of All-Electric Ships With Low-Voltage DC Hybrid Power Systems," *IEEE Transactions on Power Electronics*, vol. 28, no. 10, pp. 4525-4537, Oct. 2013
[52] T. W. Webb, T. M. Kiehne and S. T. Haag, "System-Level Thermal Management of Pulsed Loads on an All-Electric Ship," in IEEE Transactions on Magnetics, vol. 43, no. 1, pp. 469-473, Jan. 2007
[53] Georgescu, M. Godjevac and K. Visser, "Early Efficiency Estimation of Hybrid and Electric Propulsion Systems on Board

Ships,"Proc. *2017 IEEE Vehicle Power and Propulsion Conference (VPPC)*, Belfort, 2017, pp. 1-5
[54] L. N. Domaschk, A. Ouroua, R. E. Hebner, O. E. Bowlin and W. B. Colson, "Coordination of Large Pulsed Loads on Future Electric Ships," *IEEE Transactions on Magnetics*, vol. 43, no. 1, pp. 450-455, Jan. 2007
[55] J. D. Stevens, D. F. Opila, E. S. Oh and E. L. Zivi, "All-electric warship load demand model for power and energy system analysis using exogenously initiated threats," Proc. *2017 IEEE Electric Ship Technologies Symposium*, Arlington, VA, pp. 486-492
[56] X. Feng, K. L. Butler-Purry and T. Zourntos, "A Multi-Agent System Framework for Real-Time Electric Load Management in MVAC All-Electric Ship Power Systems," in *IEEE Transactions on Power Systems*, vol. 30, no. 3, pp. 1327-1336, May 2015
[57] A. Boveri, F. D'Agostino, P. Gualeni, D. Neroni and F. Silvestro, "A Stochastic Approach to Shipboard Electric Loads Power Modeling and Simulation," Proc. *2018 IEEE International Conference on Electrical Systems for Aircraft, Railway, Ship Propulsion and Road Vehicles & International Transportation Electrification Conference (ESARS-ITEC)*, Nottingham, pp. 1-6
[58] L. N. Domaschk, A. Ouroua, R. E. Hebner, O. E. Bowlin and W. B. Colson, "Coordination of Large Pulsed Loads on Future Electric Ships," IEEE Transactions on Magnetics, vol. 43, no. 1, pp. 450-455, Jan. 2007
[59] X. Feng, K. L. Butler-Purry and T. Zourntos, "Multi-Agent System-Based Real-Time Load Management for All-Electric Ship Power Systems in DC Zone Level," IEEE Transactions on Power Systems, vol. 27, no. 4, pp. 1719-1728, Nov. 2012
[60] J. Neely, L. Rashkin, M. Cook, D. Wilson and S. Glover, "Evaluation of power flow control for an all-electric warship power system with pulsed load applications," Proc. *2016 IEEE Applied Power Electronics Conference and Exposition*, Long Beach, CA, 2016, pp. 3537-3544.
[61] A. Da Rin, S. Quaia and G. Sulligoi, "Innovative concepts for power station design in all electric ships," *Proc. 2008 International Symposium on Power Electronics, Electrical Drives, Automation and Motion*, Ischia, 2008, pp. 569-573
[62] Priority of load reference: C. Chryssostomidis, J. Chalfant, D. Hanthorn, J. Kirtley and M. Angle, "Architectural Model to Enable Power System Tradeoff Studies" Massachusetts Institute of Technology, Cambridge, MA, Tech. Rep. MITSG 10-32, Jan. 2010
[63] G. Diju, P. Kangkai, C. Jianxin, S. Aidi and S. Yanyan, "Control strategy of hybrid electric ship based on improved fuzzy logic threshold," Proc. *2017 29th Chinese Control and Decision Conference*, Chongqing, pp. 6995-7000
[64] M. Farasat, A. S. Arabali and A. M. Trzynadlowski, "A novel control principle for all-electric ship power systems," *Proc. 2013 IEEE Electric Ship Technologies Symposium*, Arlington, VA, pp. 178-184
[65] A. Riccobono and E. Santi, "Stability analysis of an all-electric ship MVDC Power Distribution System using a novel Passivity-Based Stability Criterion," Proc. *2013 IEEE Electric Ship Technologies Symposium*, Arlington, VA, 2013, pp. 411-419
[66] Bolvashenkov and H. Herzog, "Use of Stochastic Models for Operational Efficiency Analysis of Multi Power Source Traction Drives," Proc. *2016 Second International Symposium on Stochastic Models in Reliability Engineering, Life Science and Operations Management*, Beer-Sheva, pp. 124-130
[67] J. Taylor and F. Hover, "High Dimensional Stochastic Simulation and Electric Ship Models," Proc. *2007 IEEE Electric Ship Technologies Symposium*, Arlington, VA, pp. 402-407
[68] Q. Yu and N. N. Schulz, "Multi-Agent Based Reconfiguration of an Electric Propulsion System for All Electric-Ships," Proc. *2007 39th North American Power Symposium*, Las Cruces, NM, pp. 153-158
[69] International Tank Towing Conference. (2002) ITTC – Recommended procedures, resistance, uncertainty analysis, example for resistance test. Revision 01 7.5-02-02-02.
[70] Principles of ship performance-Naval architecture & ocean engineering [Online] available: https://www.usna.edu/NAOE/academics/en400.php
[71] Diesel, M. A. N. (2011). Turbo. *Basic principles of ship propulsion*," MAN Diesel & Turbo, Copenhagen.
[72] A.M. Bazzi, *IEEE TEC eNewsletter*, June 2017
[73] A. Y. Mirza, W. Chen and A. Bazzi, "The impact of load sharing on multi-drive propulsion drive system efficiency," Proc. *2017 IEEE Transportation Electrification Conference (ITEC-India)*, Pune, pp. 1-5
[74] A. Ulatowski and A. M. Bazzi, "A Combinational-Logic Method for Electric Vehicle Drivetrain Fault Diagnosis," *IEEE Transactions on Industry Applications*, vol. 52, no. 2, pp. 1796-1807, March-April 2016
[75] J. J. Cathey, R. K. Cavin and A. K. Ayoub, "Transient Load Model of an Induction Motor," *IEEE Transactions on Power Apparatus and Systems*, vol. PAS-92, no. 4, pp. 1399-1406, July 1973